EFDA-JET-CP(06)04-03

S. Sadakov, Ed. Bondarchuk, N. Doinikov, T. Hirai, B. Kitaev,
N. Kozshukhovskaya, I. Maximova, Ph. Mertens, O. Neubauer,
T. Obidenko and JET EFDA contributors

# Detailed Electromagnetic Analysis for Design Optimization of a Tungsten Divertor Plate for JET

# Detailed Electromagnetic Analysis for Design Optimization of a Tungsten Divertor Plate for JET

S. Sadakov[1], Ed. Bondarchuk[2], N. Doinikov[2], T. Hirai[3], B. Kitaev[2], N. Kozshukhovskaya[2], I. Maximova[2], Ph. Mertens[1], O. Neubauer[1], T. Obidenko[2] and JET EFDA contributors*

*[1]Institut für Plasmaphysik, Forschungszentrusm Jülich, Association EURATOM-FZJ, Trilateral Euregio Cluster, D-52425 Jülich, Germany*

*[2]SINTEZ Scientific Technical Center, D.V. Efremov Scientific Research Institute of Electrophysical Apparatus, RUS-189632 St. Petersburg, Russia*

*[3]Institut für Werkstoffe und Verfahren der Energietechnik, Forschungszentrum Jülich, Association EURATOM-FZJ, D-52425 Jülich, Germany*

** See annex of J. Pamela et al, "Overview of JET Results", (Proc. 20th IAEA Fusion Energy Conference, Vilamoura, Portugal (2004).*

Preprint of Paper to be submitted for publication in Proceedings of the SOFT Conference,
(Warsaw, Poland 11th – 15th September 2006)

**ABSTRACT.**

The ITER-Like Wall project (ILW) at JET aims at replacing Carbon Fiber Composite (CFC) on plasma-facing surfaces by tungsten and beryllium, which are relevant to the ITER design. The original design of the JET divertor, with CFC tiles, has quite high eddy-current related loads. Tungsten has a much higher electrical conductivity than CFC, and this does not allow a simple replacement of the CFC with solid tungsten in the original design.

So called fishbone- or tree-like shapes, avoiding large loops of eddy currents, have been proposed for the tungsten components and supporting structures. These shapes reduce the eddy current loads drastically and provide well defined paths for the Halo current.

This report describes how the design of the supporting structures is driven by electromagnetic considerations. Analytical and numerical techniques are combined and cross-checked. A study has undertaken for two variable orthogonal magnetic fields, for two cases of halo current, with three orthogonal background magnetic fields. Then the worst load combinations were identified and used for the calculation of the forces and stresses in fixtures.

## 1. DESIGN DESCRIPTION FOR PRESENTLY USED & NEWLY DEVELOPED JET DIVERTOR

The ITER-Like Wall Project (ILW) at JET [1, 2] aims at replacing the Carbon Fiber Composite (CFC) on plasma-facing surfaces by tungsten (W) and beryllium (Be), which are relevant to the ITER design. One of the R&D projects in the ILW Project is to develop bulk W components as a replacement for the CFC Load-Bearing Septum Replacement Plates (LB-SRP) [3, 4].

The centrally located part of the original JET divertor consists of 48 “Load-Bearing Septum Replacement Plates” (LB-SRP). Each includes two large CFC tiles ($250 \times 170 \times 40\text{mm}^3$) and two small CFC tiles ($160 \times 85 \times 25\text{mm}^3$). The tiles are attached on two superimposed Inconel frames. Electromagnetic (EM) analysis for the original design has shown that it can accomodate just marginally the eddy-current related loads. Tungsten has relatively high electrical conductivity, exceeding that of CFC by about two orders of magnitude (at $80^{o}$C, taken as design input), and this does not allow the principle of the original design to be kept with a simple replacement of the CFC by solid tungsten. Instead a total redesign of the LB-SRP including the supporting structures has been necessary. This has increased significantly the overall R&D effort.

A solution has been proposed to employ an assembly of thin ($6 \times 60 \times 40\text{mm}^3$) W lamellae on a fishbone shaped supporting structure, which excludes large contours of eddy currents and provides well-defined Halo current paths (Fig.1) [5-6].

The detailed features of the design are summarized below.

- All lamellae are grouped in pairs, which are separated by insulated spacers.
- Within each pair, two lamellae are interconnected by non-insulated T-shaped spacer.
- T-spacers are used for attachment and for providing a path for the halo current.

– Lamellae with spacers are assembled in eight stacks, about $170 \times 60 \times 40$ mm$^3$ each.
– Each stack is compressed by two tie rods with sufficient elastic properties.
– Each stack is attached to a beam. All beams are elongated toroidally and called wings.
– All eight wings are integral with a middle part, elongated in the radial direction.
– Each wing has a foot stepping on a base plate and providing a path for the halo current.
– Two additional shorter wings are located under two top wings for structural purposes.
– The middle part, all wings and feet, are made as a monolithic Inconel piece, called a wedge.
– The adapter locates between the wedge and the base plate and has a cross-like shape.

This paper presents major results of the transient electromagnetic (EM) analysis aimed at optimizing the design of the JET divertor with solid tungsten components.

## 2. CALCULATION TECHNIQUE AND TASK DEFINITION

This task has been made in parallel to a complete Finite Element (FE) analysis with the ANSYS model [7]. Results were cross-checked. Because of the large number of parts, a complete FE model does not allow a sufficiently detailed mesh within each lamella. This restricts the accuracy of the EM simulation, and a recheck with other methods appeared to be necessary.

In this paper, the numerical studies are limited to the essential components such as pair of lamellae or a wing, etc. The resistive approximation is proven to be valid for all components. The numerical results were used to adjust coefficients in formulas, employed for the practical calculations described below.

The divertor was simplified to a set of effective rectangular bricks or lanes and each of them was analyzed with formulas for a "resistive pattern" of eddy currents. For example, each lamella was split in three zones, with different formulas used for each zone and for each vector of a variable magnetic field. The formulas used adjustment coefficients which are chosen by comparison with the numerical results for selected components.

The following currents and load components were accounted, and sum forces found:

– eddy currents induced by the variation of radial and vertical magnetic fields (100T/s each);
– global toroidal eddy current (fig.4), induced by the variation of the poloidal magnetic flux,
– eddy-current related loads in three orthogonal background magnetic fields (1T, 1T, 4.6T);
– halo current pattern for two cases (entering side surfaces of two top stacks, 9kA/stack, or exiting face surfaces of all eight stacks, 2.25kA/stack to) and related loads;
– load superposition and the worst load combinations (figs. 3, 5, 8, 9);
– forces and stresses in the fixtures for the worst load combinations (figs. 3, 8, 9).

The plasma current is co-directional with the toroidal field, and both may be switched while keeping

the helicity unchanged. This gives arbitrary directions of the radial and vertical magnetic fields, their derivatives, and the related EM loads.

## 3. EM LOADS FOR LAMELLAE AND FOR THE STACKS, AND FORCES IN THE LINKS AND TIE RODS

Figure 2 show the local coordinates, magnetic fields and eddy current related loads for a pair of lamellae (regular Vs. outer) and a stack of lamellae. Fig. 3 shows the detaching EM loads (sum of the eddy and halo) and pre-stress forces required for one T-spacer and one tie rod.

In this specific design each outer lamella encloses the nuts and washers of the tie rods. This makes the outer lamellae thicker than a regular one (10mm instead of 6mm). For a single lamella, the torque moments $M_y$ and $M_n$ are in near a cubic dependence on thickness. Thus the load created in one outer lamella is a factor of 4 higher then for the regular one. This means that the thickness of the outer lamella defines the pre-tension force for the tie rods. A higher pre-tension leads to the need for larger nuts and washers which, for their allocation, need thicker outer lamellae. This unfavorable "positive feedback" can destroy the design.

The first practical conclusion is to define and fulfill a strict design limit for the thickness of the outer lamella.

## 4. EDDY CURRENT LOADS FOR THE WEDGE, AND SUM FOR THE STACKS, WEDGE AND ADAPTOR

For variation of the normal magnetic field, the dominant EM load is the radial torque moment $M_y$ (fig.4, left side). It defines the pre-tension force for the bolts. In the original divertor it is 610Nm for the wedge alone and 1050 Nm with CFC tiles mounted on it. For the newly proposed fishbone design a large current loop is cut in 8 local loops with a smaller linked flux and a larger resistance. This reduces the torque moment $M_y$ by more than one order of magnitude.

Thus the second practical conclusion is that a change to the fishbone shape reduces EM loads drastically, with the best results for an equal width of all the wings.

For variation of the radial magnetic field, the so called "transport" eddy current flows through a toroidal loop formed by all 48 wedges interconnected via the CFC base plate (fig.4, right side). The transport current was simulated numerically and found to be 9.6kA (sum for the wedge). This is comparable with the peak halo current (9kA/stack), and creates loads of a similar scale: $M_n$=360Nm. The third practical conclusion is that for the components resembling the JET divertor, the design should take into account the EM loads caused by the described transport eddy current.

## 5. HALO CURRENT AND RELATED LOADS

Figure 6 shows two patterns of the halo current: either entering the side surfaces of two top stacks (left), or exiting the face surfaces of all stacks (right). The main component of halo-related loads is a radial force. This force is almost independent of the design since it is defined by the net Halo

current and the height of the divertor. Another component, the vertical force, varies with the effective length of the radial current path. However it acts only downward and is thus irrelevant to the design of the attachments.

The halo-related force created at the foot of the top wings (fig.6, left side) tends to twist the upper wing. This wing torsion caused too high deformations, but this has been resolved with the addition of two shorter wings (fig.1). They convert the torsion into an in-plane bending. Short wings create closed loops, which contradict a principle of the fishbone design. The related penalty was studied numerically and found to be modest. The reason originates from the nature of the transport current, which tends to flow in a path closest to the plasma, and less then 10% deviates into the short wings.

The fourth practical conclusion is that the toroidal branches in the fishbone design may be shunted by parallel beams, if they are considered to be necessary for structural purposes. The penalty is modest due to the nature of the transport current.

One component of the halo-related loads is very sensitive to the location of the feet. This is a torque moment around the vertical axis. Figure 7 explains the reason: the load changes its sign when the span between feet equals ~58% of the toroidal size of the wedge.

The fifth practical conclusion is that the contact elements passing the halo current should be located on a span equal ~58% of the toroidal size, in order to compensate the normal torque moment which is caused by the halo current.

## 6. REQUIRED PRE-TENSION FORCES FOR THE BOLTS AND LATERAL FORCES APPLIED TO THE DOWELS

The wedge is attached to the adapter by two bolts located in the middle line (fig.8). The radial torque moment (shown in fig. 5) is a dominant load, which defines the detaching force (fig.8, left) and accordingly the required bolts pre-tension force (fig.8, right).

Figure 9 Shows the cross-like adapter and the forces applied to it. The lateral forces (right side) are mostly halo-defined and thus not sensitive to design details. However, based on this study the dowels diameter has been increased to 9mm, to ensure sufficient reserve factors, ~2.0 and ~3.0 for the side dowels and for the central dowel, respectively.

The fishbone shape cuts the detaching force in several folds, and accordingly relaxes the pre-tension force. For the original divertor a single bolt (M12) is pre-tensioned with 27kN, and for the fishbone design this force went down to 7kN, and shared by two bolts: M12 and M8, as 5.0kN and 2.0kN (fig.8, right). The pretension forces shown in Fig. 8, 9 were taken as input in [6, 7], and increased by ~20% to get a feasible margin for detachment.

## CONCLUSIONS

The fishbone shape allows the realization of a divertor tile design with bulk tungsten for the JET central divertor tile row (LBSRP). The electromagnetic analysis performed for all components has

resulted in five key practical recommendations, which formed the basis for the new design. The pre-tension forces of the bolts remain to be defined by eddy currents, but were reduced in several folds, allowing sufficient reserve factors and relaxing also the load on the underlying CFC plate. The lateral forces on the dowels are defined by halo currents and can't be reduced by any design modifications, but an adequate diameter of the dowels has been chosen based on this study.

**ACKNOWLEDGEMENTS**

The authors are indebted to the TEXTOR team for fruitful collaboration and communication on this design and analysis task and to the JET operator and ILW project team for information on the design features and parameters of the presently used JET divertor. Productive discussions with B. Schweer, V. Philipps, U. Samm and input provided by H. Altmann and V. Riccardo are gratefully acknowledged. This work, supported by the European Communities under the contract of Association between EURATOM/FZJ, was carried out within the framework of the European Fusion Development Agreement. The views and opinions expressed herein do not necessarily reflect those of the European Commission.

**REFERENCES**

[1]. G. F. Matthews, T. Hirai, A. Lioure, A. Loving, H. Maier, J. Pamela, V. Philipps, G. Piazza, V. Riccardo, M. Rubel, E. Villedieu for the ITER-like Wall Project Team, "ITER-like Wall Project Overview", to be presented in PFMC-11, Greifswald Germany, October 2006.

[2]. J. Pamela, et al., "An ITER-like Wall for JET", presented at 17th international conference on plasma surface interaction in controlled fusion devices, Hefei China, 22-26 May 2006.

[3]. G. Piazza, G. F. Matthews, J. Pamela, H. Altmann, J. P. Coad, T. Hirai, A. Lioure, E. Villedieu, H. Maier, P. Mertens, V. Philipps, M. Rubel and collaborators of the JET ITER-like Project, "The ITER-like Wall Project", presented at ICFRM-12, Santa Barbara US, December 2006.

[4]. T. Hirai et al., "R&D on full tungsten divertor and beryllium wall for JET ITER-like Wall Project", Fusion Engineering and Design, present issue.

[5]. Ph. Mertens and the JET W/bulk team, Chap. 3 *in* Conceptual design for a tungsten bulk LB-SRP, Final Report, T. Hirai and Ph. Mertens *edd.,* March 2006, (internal JET/EFDA document)

[6]. Ph. Mertens, T. Hirai, O. Neubauer, V. Philipps, S. Sadakov, U. Samm, B. Schweer, JET-EFDA contributors, "Conceptual design for a bulk tungsten divertor tile in JET", in these proceedings.

[7]. A. Borovkov, A.Gaev, A. Nemov, "3-D finite element coupled field analysis of the JET LB-SRP divertor element", in these proceedings.

| Components: | Stacks | Wedge | Sum S+W | Adapter | Sum S+W+A |
|---|---|---|---|---|---|
| $M_T$ | 48.8 (17 ) | 64 (183) | 113 (200) | 31 (100) | 143 (300) |
| $M_R$ | 151 (440) | 124 (610) | 275 (1050) | 31 (570) | 306 (1620) |
| $M_Z$ | 127 (50) | 272 (33+340*) | 399 (83) | 12 (7) | 411 (90+340*) |

(*) This accounts effect of the transport current, which was not indicated for the original design.

*Table 1: Eddy current related torque moments. Values in brackets are for the original JET divertor, calculated with the same input data.*

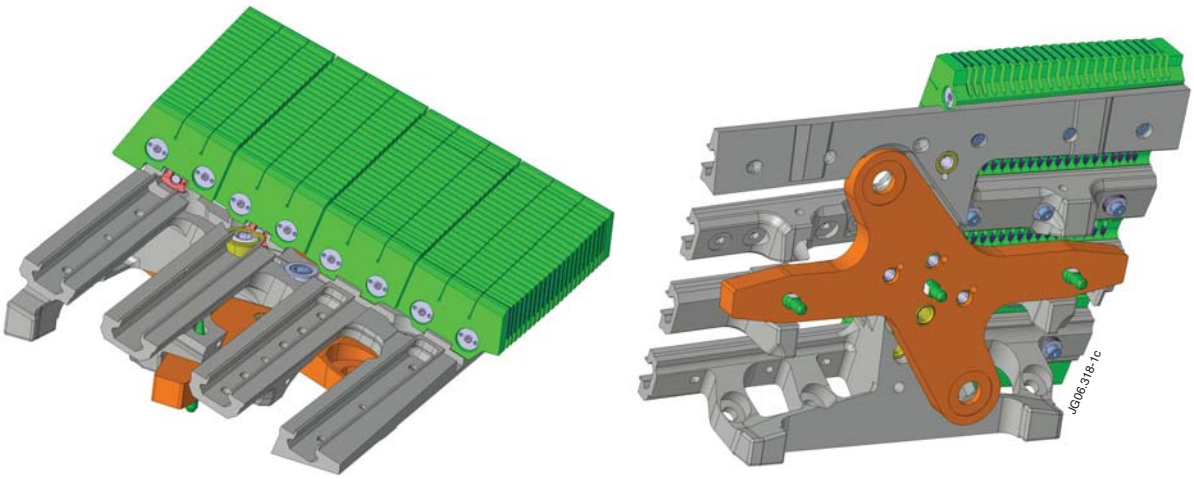


*Figure 1: Bulk W lamellae component with fishbone-shaped supporting structure: views from the top (left) and bottom (right), with four stacks removed to show the wings. W lamellae are in green, the wedge is in grey and the adapter is in orange.*

*Mn= +/-(0.9 – 1.9) Nm/pair (regular Vs. outer)* *Mn= +/- 11 Nm/stack*

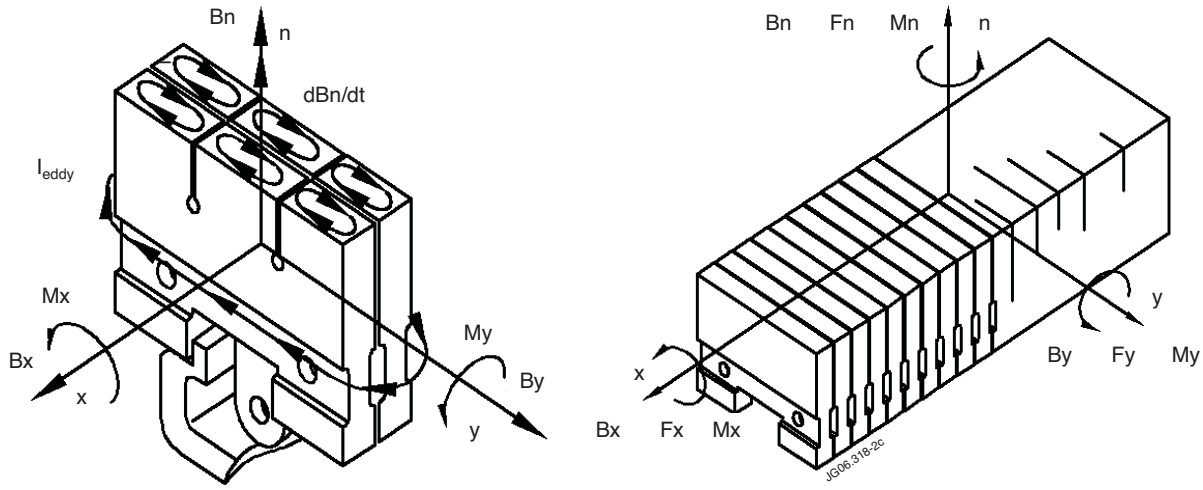


*Mx=+/-(0.45-1.0)Nm/pair My= +/-(1.25-2.85)Nm/pair Mx=+/-6Nm/stack My=+/-16Nm/stack*

*Figure 2: Directions of magnetic fields and loads by eddy currents for a pair of regular or outer lamellae and for an average stack (eddy currents are shown for only $dB_n/dt$, but loads are for all components).*

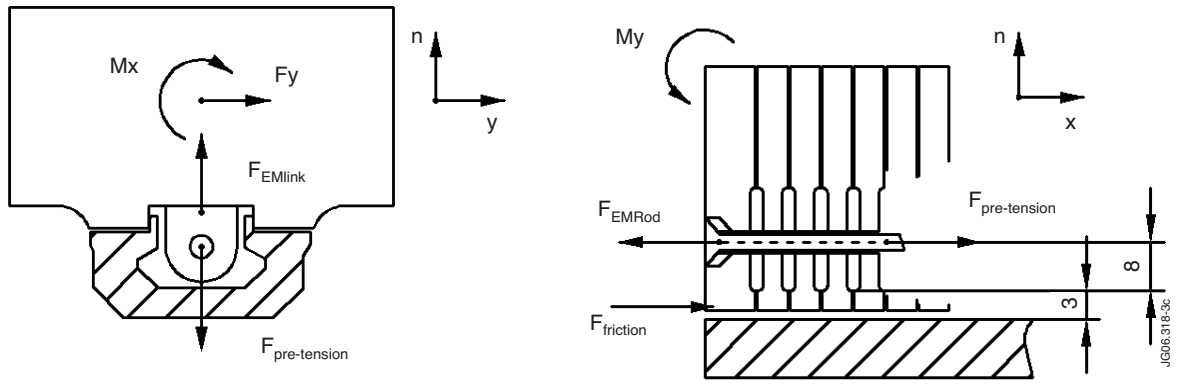


*$F_{EM\_link}$= 30 N (regular), or 75 N (outer);* *$F_{EM\_rod}$ = 0.15 kN/rod plus effect of friction;*
*$F_{PreTens\_link}$= 60 N (regular), or 150N (outer)* *$F_{PreTens\_Rod}$ = 0.5 kN/rod or, better 1.0 kN/rod*

*Figure 3: Detaching EM loads and pre-tension forces for a link and a tie rod.*

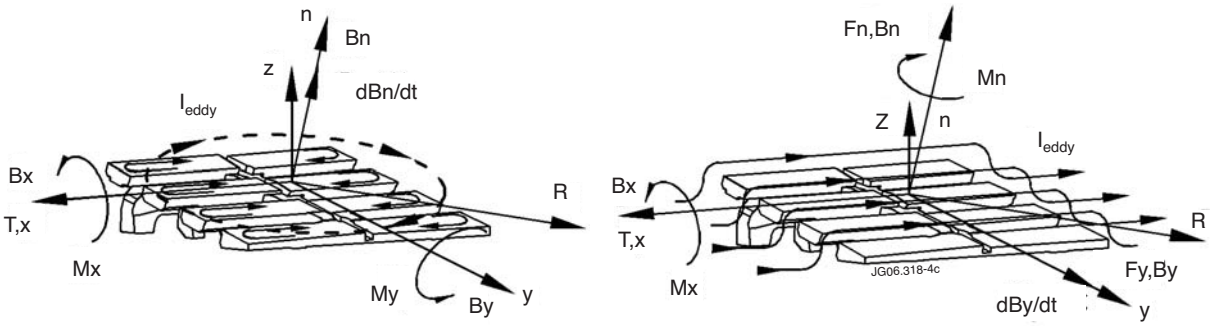


*Figure 4: Components of magnetic fields, eddy currents and EM loads on the wedge for cases of variation of the normal (left) and radial (right) magnetic fields.*

$$S + W + A = (S+W+A)$$
$$M_Z = 127 + 272 + 12 = 411\ Nm\ (M_{Z\_CFC} = 430)$$

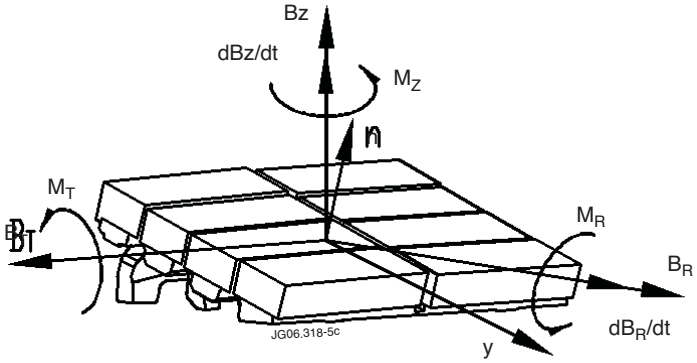


$M_T = 49 + 64 + 31 = 143\ Nm\ (M_{T\_CFC} = 300)$ $M_R = 151 + 124 + 31 = 306\ Nm\ (M_{R\_CFC} = 1620)$

*Figure 5: Eddy current related torque moments for the stacks (S), wedge (W), adapter (A) and the sum.*

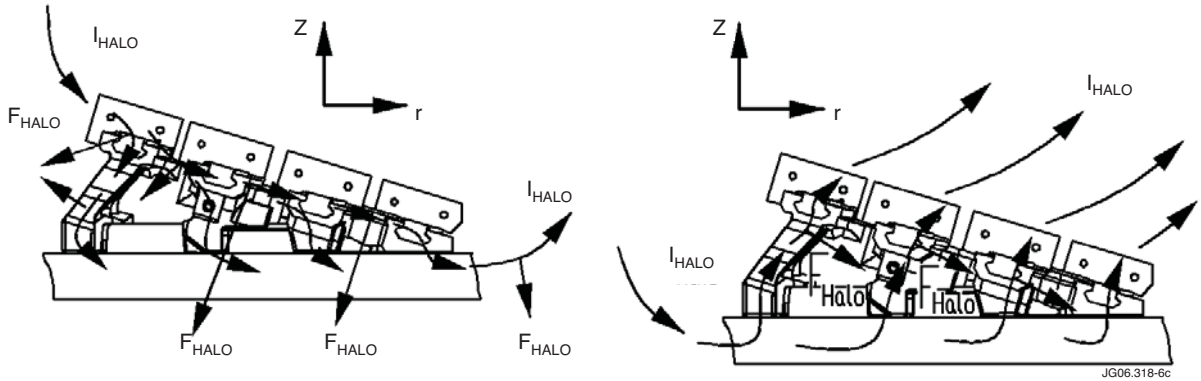


$F_{Rhalo} = -8160\ N;\ F_{Zhalo} = -10800\ N$ $F_{Rhalo} = +6950\ N;\ F_{Zhalo} = -760\ N$

*Figure 6: Two patterns for the halo current: entering side surfaces of two top stacks (left) or exiting front surfaces of all eight stacks (right).*

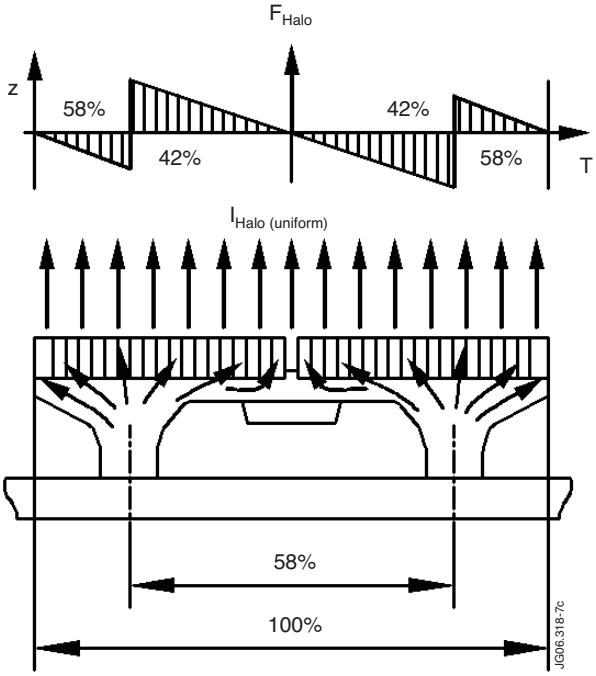


*Figure 7: Pattern of Halo current along two wings, and profiles of the forces $F_R$ and $F_Z$.*

*Detaching forces caused by EM loads* *Pre-stress and reaction forces applied to the wedge*

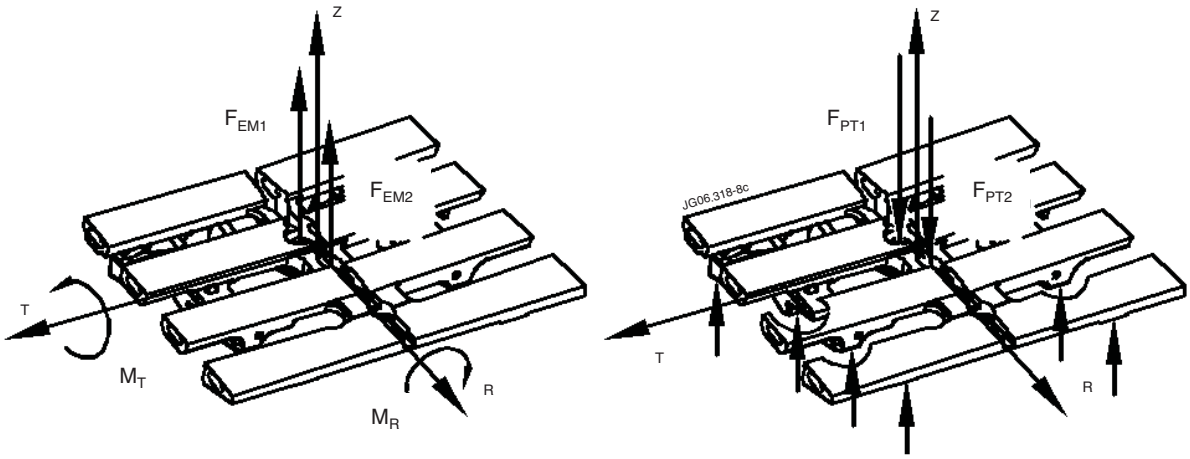


$F_{EM1} + F_{EM2} = 5.0$ *kN* $F_{PT1} + F_{PT2} = -7.0$*kN* $F_{react} = (0.75\text{-}1.0)$*kN each*

*Figure 8: Detaching forces caused by EM torque moments, and required pre-stress forces for the wedge.*

*Vertical forces applied to the adapter* *Lateral forces applied to the adapter*

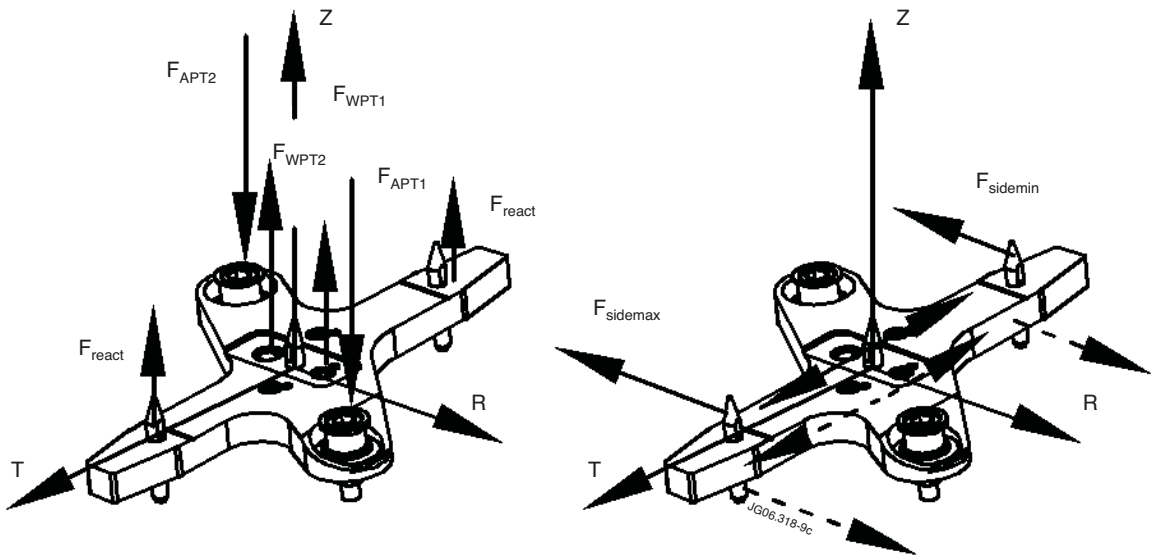


$F_{APT1}$= -4.5kN; $F_{APT2}$= -4.5kN; $F_{SideMax}$= -6.12kN; $F_{centr}$= +/-4.05kN; $F_{SideMin}$= -3.2kN

*Figure 9: Cross like adapter and forces applied to it: by bolts (left) and on dowels (right)*